Wärme- und Stoffübertragung 14, 157-164 (1980)

Wärme- und Stoffübertragung
Thermo- and Fluid Dynamics

Turbulent Natural Convection Over a Slender Circular Cylinder

T.Y. Na and J.P. Chiou

Abstract. The transverse-curvature effect on the heat transfer in the turbulent natural convection flow from the outer surface of a slender vertical circular cylinder is studied by an improved integral method for various values of Prandtl numbers and for various values of a transverse curvature parameter.

Turbulente natürliche Konvektion an einem schlanken Kreiszylinder

Zusammenfassung. Der Einfluß der Querkrümmung auf die Wärmeübertragung von der Außenoberfläche eines dünnen senkrechten Kreiszylinders in die turbulente, natürliche Konvektionsströmung wird mittels eines verbesserten Integral-Verfahrens für verschiedene Werte der Prandtl-Zahlen und der Querkrümmungsparameter untersucht.

Nomenclature

c_p	heat capacity, kcal/kg°C
g	gravitational acceleration
L, m, n	constants
q	heat flux, kcal/m^{2}h
r_0	radius of cylinder
T	temperature, °C
u	velocity in x-direction, m/h
u_β	velocity head due to buoyancy, m/h $u_\beta^2 = \int g\beta(t - t_\infty)dx$
v	velocity in y-direction, m/h
x	flow direction, m
y	normal direction to flow, m
r	$r_0 - y$
v^*	friction velocity, $\sqrt{\tau_w/\rho}$
u^+	dimensionless velocity, $u^+ = u/v^*$
T^+	dimensionless temperature, $T^+ = (T_w - T)c_p g\tau_w / q_w v^*$
x^+	dimensionless coordinate, $x^+ = xv^*/\nu$
y^+	dimensionless coordinate, $y^+ = yv^*/\nu$
Re_x	local Reynolds number, $Re_x = ux/\nu$
Nu_x	local Nusselt number, $Nu_x = hx/k$
Pr_x	Prandtl number, $\mu C_p/k$
Gr_x	Grashof number, $Gr_x = g\beta x^3(T_w - T_\infty)/\nu^2$
Ra_x	Rayleigh number, $Ra_x = Gr_x Pr$

Greek Symbols

β	body expansion coefficient, 1/°C
δ	boundary-layer thickness, m
ε	eddy diffusivity, m^2/h
θ	dimensionless temperature
ν	kinematic viscosity, m^2/h
ρ	density, kg/m^3
τ	shear stress, N/m^2
δ^+	dimensionless boundary-layer thickness, $\delta^+ = v^*\delta/\nu$

Subscripts

w	wall condition
∞	condition far from the wall

1 Introduction

When the radius of a circular cylinder is of the same order-of-magnitude as the thickness of the boundary layer, the transverse-curvature effect becomes very important. The resultant changes in the skin friction and the heat transfer characteristics are no longer negligible. Many studies have been made on the effect of transverse curvature on the forced convection over slender circular cylinders. These include both laminar and turbulent flows. For the case of natural convection over such bodies, however, published results are limited to the case of laminar flows [1-3]. It is, therefore, the purpose of this paper to study the natural convection over a slender curcular cylinder where the flow is in the turbulent regime. The method to be used in this analysis is the one originally developed by Kato, Nishiwaki and

0042-9929/80/0014/0157/$ 1.60

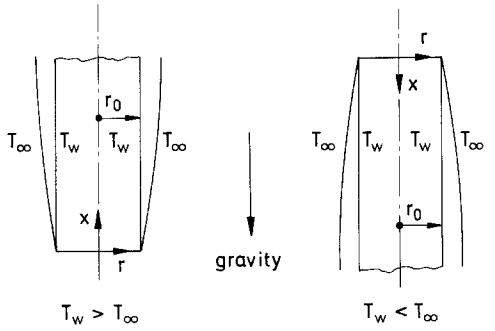

Fig.1. Schematic Diagram of the Cylinder

Hirata [4], which is basically an improved integral method. The method is very simple and has been proved (in reference 4 as well as in the present paper) to be quite accurate for a large range of Prandtl numbers. Due to lack of both theoretical and experimental works on the natural convection flow in the turbulent regime for geometries other than the semi-infinite flat plate, solutions obtained from the present analysis offer not only useful heat transfer data but also some insight into turbulent natural convection flows over other geometries.

2 Analysis

The boundary layer equations for natural convection flow of incompressible fluids over an isothermal vertical cylinder (Fig.1) can be written as:

$$\frac{\partial}{\partial x}(ru) + \frac{\partial}{\partial r}(rv) = 0 \tag{1}$$

$$\rho\left(u\frac{\partial u}{\partial x} + v\frac{\partial u}{\partial r}\right) = \rho g\beta(T - T_\infty) + \frac{1}{r}\frac{\partial}{\partial r}(r\tau) \tag{2}$$

$$\rho c_p\left(u\frac{\partial T}{\partial x} + v\frac{\partial T}{\partial r}\right) = -\frac{1}{r}\frac{\partial}{\partial r}(rq) \tag{3}$$

subject to the boundary conditions:

$r = r_0$: $u = 0$, $v = 0$, $T = T_w$

$r = \infty$: $u = 0$, $T = T_\infty$

The fluid properties are assumed to be constant except the change of density inside the boundary layer which creates the buoyancy force. The boundary layer is assumed to be turbulent starting from the leading edge ($x = 0$) of the cylinder.

Similar to Kato, Nishiwaki and Hirata [4], the integral form of the boundary layer equations will now be derived. From Eq.(1), we get:

$$rv = -\int_{r_0}^{r} \frac{\partial(ru)}{\partial x}dr \tag{4}$$

which can be substituted into Eq.(2) and the resulting equation integrated over the boundary layer thickness. We then get:

$$r_0\tau_w = \rho\int_{r_0}^{r_0+\delta} g\beta r(T - T_\infty)dr - \rho\int_{r_0}^{r_0+\delta}\frac{\partial(ru^2)}{\partial x}dr \tag{5}$$

If a function u_β is defined such that

$$g\beta r(T - T_\infty) = \frac{\partial r u_\beta^2}{\partial x} \tag{6}$$

Equation (5) can be written as:

$$r_0\tau_w = \rho\frac{d}{dx}\int_{r_0}^{r_0+\delta} r(u_\beta^2 - u^2)dr \tag{7}$$

Next, Eq.(4) can be substituted into Eq.(3) and the resulting equation integrated over the thermal boundary thickness. We then get:

$$r_0 q_w = \rho c_p\frac{d}{dx}\int_{r_0}^{r_0+\delta_t} ru(T - T_\infty)dr \tag{8}$$

In terms of the dimensionless variables defined by:

$$x^+ = \frac{xv^*}{\nu},\quad y^+ = \frac{yv^*}{\nu},\quad u_\beta^+ = \frac{u_\beta}{v^*},\quad u^+ = \frac{u}{v^*},$$

$$T^+ = \frac{c_p\tau_w(T_w - T)}{q_w v^*} \tag{9}$$

the momentum integral equation, Eq.(7), and the energy integral equation, Eq.(8), become:

$$1 = \frac{d}{dx^+}\int_0^{\delta^+}\left(1 + \frac{y^+}{r_0^+}\right)(u_\beta^{+2} - u^{+2})dy^+$$

$$1 = \frac{d}{dx^+}\int_0^{\delta_t^+}\left(1 + \frac{y^+}{r_0^+}\right)u^+(T_\infty^+ - T^+)dy^+$$

which can be integrated to give:

$$x^+ = \int_0^{\delta^+} \left(1 + \frac{y^+}{r_0^+}\right)(u_\beta^{+2} - u^{+2})dy^+ \tag{10}$$

$$x^+ = \int_0^{\delta_t^+} \left(1 + \frac{y^+}{r_0^+}\right) u^+(T_\infty^+ - T^+)dy^+ \tag{11}$$

The improvement made by Kato, Nishiwaki and Hirata [4] over the classical integral method of Eckert and Jackson [5] is that, instead of assuming the velocity and the temperature profiles, they are derived by simplifying the momentum and the energy equations and by assuming the eddy viscosity and the turbulent Prandtl number to be:

$$\frac{\varepsilon}{\nu} = 0.4y^+[1 - \exp(-0.0017y^{+2})] \tag{12}$$

$$Pr_t = 1 \tag{13}$$

Details are given below:

First, the inertial terms in Eq.(2) and the convective terms in Eq.(3) are dropped, which gives:

$$\rho g\beta(T - T_\infty) + \frac{1}{r}\frac{\partial}{\partial r}(r\tau) = 0 \tag{14}$$

$$\frac{\partial}{\partial r}(rq) = 0 \tag{15}$$

Let us first consider Eq.(14). Integrating over r and applying the boundary condition

$$r = r_0 : \tau = \tau_w$$

Equation (14) becomes:

$$r\tau + \rho g\beta \int_{r_0}^{r} r(\tau - t_\infty)dr = r_0\tau_w$$

which, upon applying Eq.(6), becomes:

$$r\tau + \rho \int_{r_0}^{r} \frac{\partial(ru_\beta^2)}{\partial x} dr = r_0\tau_w \tag{16}$$

Following Kato, Nishiwaki and Hirata [4], we assume

$$\frac{\partial(ru_\beta^2)}{\partial x} = \frac{ru_\beta^2}{x} \tag{17}$$

Equation (16) becomes:

$$r\tau + \rho \int_{r_0}^{r} \frac{ru_\beta^2}{x} dr = r_0\tau_w \tag{18}$$

With the assumption in Eq.(17), Eq.(6) becomes:

$$\frac{ru_\beta^2}{x} = g\beta r(T - T_\infty) \tag{19}$$

On the cylinder surface, $r = r_0$, $u_\beta = u_{\beta w}$. We get:

$$\frac{r_0 u_{\beta w}^2}{x} = g\beta r_0(T_w - T_\infty) \tag{20}$$

Based on Eqs.(19) and (20), it can be shown that:

$$\frac{ru_\beta^2}{x} = \frac{r_0 u_{\beta w}^2}{x}\left(1 + \frac{y^+}{r_0^+}\right)\left(1 - \frac{T^+}{T_\infty^+}\right) \tag{21}$$

which, together with:

$$\frac{\tau}{\tau_w} = \left(1 + \frac{\varepsilon_m}{\nu}\right)\frac{\partial u^+}{\partial y^+} \tag{22}$$

reduces Eq.(18) to:

$$\left(1 + \frac{y^+}{r_0^+}\right)\left(1 + \frac{\varepsilon_m}{\nu}\right)\frac{\partial u^+}{\partial y^+} + \frac{(u_{\beta w}^+)^2}{x^+} \times \int_0^{y^+} \left(1 + \frac{y^+}{r_0^+}\right)\left(1 - \frac{T^+}{T_\infty^+}\right)dy^+ = 1$$

Which can be integrated to five:

$$u^+ = \int_0^{y^+} \frac{\left[1 - \frac{(u_{\beta w}^+)^2}{x^+}\int_0^{y^+}\left(1 + \frac{y^+}{r_0^+}\right)\left(1 - \frac{T^+}{T_\infty^+}\right)dy^+\right]}{\left(1 + \frac{y^+}{r_0^+}\right)\left(1 + \frac{\varepsilon_m}{\nu}\right)} dy^+ \tag{23}$$

Next, Eq.(15) gives:

$$rq = r_0 q_w \tag{24}$$

Since for turbulent flows,

$$q = -\rho c_p(\alpha + \varepsilon_m)\frac{\partial T}{\partial y} \tag{25}$$

Equation (24), in terms of the dimensionless quantities defined in (9), becomes,

$$1 = \frac{1}{Pr}\left(1 + \frac{y^+}{r_0^+}\right)\left(1 + \frac{Pr}{Pr_t}\,\frac{\varepsilon_m}{\nu}\right)\frac{dT^+}{dy^+} \tag{26}$$

Which can be integrated to give:

$$T^+ = \int_0^{y^+} \frac{Pr\, dy^+}{\left(1 + \frac{y^+}{r_0^+}\right)\left(1 + \frac{Pr}{Pr_t}\,\frac{\varepsilon_m}{\nu}\right)} \tag{27}$$

With u^+ and T^+ found from Eqs.(23) and (27), they can be substituted back into Eqs.(10) and (11). This completes the derivation of the equations necessary for the solution of the problem.

It should be noted that the ratio y^+/r_0^+ in Eqs.(10), (11), (23) and (27) represent the relative importance of the transverse curvature. Let us re-write the factor $(1 + y^+/r_0^+)$ as:

$$1 + \frac{y^+}{r_0^+} = 1 + \frac{1}{Gr_0^{1/3}}\,\lambda^{\frac{1}{3}}\,y^+ = 1 + \xi\lambda^{\frac{1}{3}}\,y^+ \tag{28}$$

where

$$Gr_0 = \frac{g\beta(T_w - T_\infty)r_0^3}{\nu^2}\,, \quad \xi = Gr_0^{-1/3} \text{ and } \lambda = \frac{(u_{\beta w})^2}{x^+}$$

For cylinders with radius r_0 very large compared with the boundary layer thickness, the ratio becomes negligible, i.e.,

$$\left(1 + \frac{y^+}{r_0^+}\right) \cong 1$$

Equations (10), (11), (23) and (27) then become identical to the equations for the turbulent natural convection over a semi-infinite plate, treated by Kato, Nishiwaki and Hirata [4].

This is consistent with the physical observation that when the radius of the cylinder is large, the effect of transverse curvature is negligible and the boundary layer is the same as that over a semi-infinite plate.

The parameter ξ is therefore seen as the parameter indicating the effect of transverse curvature. Since it is inversely proportional to the radius of the cylinder, the effect is more pronounced for cylinders with smaller radius. Numerical solutions for a few values of ξ will be presented in a later section.

Even though the solution of the above equations involve only integration, an iteration process is needed [4]. The steps followed will now be outlined briefly. For a given Pr and ξ, a value of δ^+ is first chosen. With ε_m/ν and Pr_t given by Eqs.(12) and (13), Eq.(27) can be integrated from $y^+ = 0$ to $y^+ = \delta^+$. With $T^+(y^+)$ known, a value of the ratio

$$\lambda = \frac{(u^+_{\beta w})^2}{x^+} \tag{29}$$

is assumed and the velocity distribution can be obtained from $y^+ = 0$ to $y^+ = \delta$ by integrating Eq.(23). Different values of λ are assumed until the values of x^+ from both Eqs.(10) and (11) agree with each other. Successive approximations are guided by the requirement that u^+ equals to zero at $y^+ = \delta^+$.

The above scheme gives a pair of values of λ and x^+ for one value of δ^+. The thermal boundary layer thickness, δ_t^+, and the temperature at the edge of the thermal boundary layer, T^+_∞, can be identified by an inspection of the numerical results.

It can be shown that Eq.(20) gives

$$Gr_x = \frac{g\beta(T_w - T_\infty)x^3}{\nu^2} = \lambda x^{+3} \tag{30}$$

Also, the local Nusselt number can be written as

$$Nu_x = \frac{hx}{k} = \frac{q_w x}{(T_w - T_\infty)k} = \frac{Pr\, x^+}{T^+_\infty} \tag{31}$$

It is now clear that we have found one pair of the data required in a tabulation of Nu_x - vs - Gr_x.

Other values of δ^+ can be assigned and the above scheme repeated. A table of Nu_x - vs - Gr_x for a given pair of values of Pr and ξ can now be generated.

3 Results and Discussions

Based on the method outlined above, numerical solutions have been generated for Prandtl numbers of 0.7,

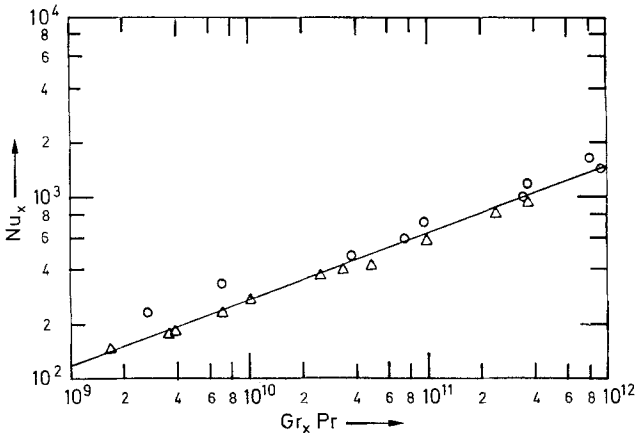

Fig.2. Experimental data vs theoretical results based on present method. (Pr = 1.0)
o Jakob [7] Δ Saunders [8]

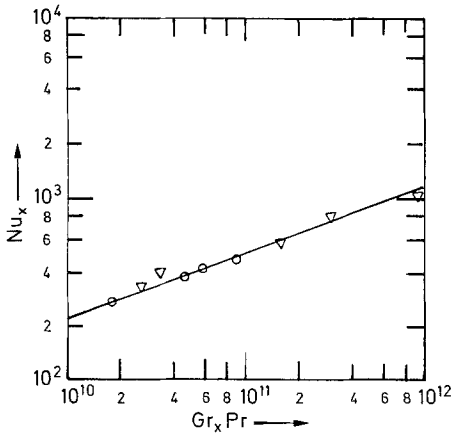

Fig.4. Experimental data vs theoretical results based on present method. (Pr = 40)
Fujii [9] Touloukian et al.[10]

1.0, 10, and 100 and for a few values of ξ. For the case of $\xi = 0$, solutions for three more Prandtl numbers (Pr = 5, 40 and 60) are obtained for the purpose of comparing with experimental data.

Experimental data for turbulent natural convection over circular cylinders are available only for the case of large cylinder radius where the effect of transverse curvature is negligible [6]. For this case, the boundary layer flow is the same as the flow over a semi-infinite flat plate. Experimental data from references 7, 8, 9 and 10 can, therefore, be used along with those from reference 6.

Figures 2 through 6 show the local Nusselt number, Nu_x, based on the present integral method as compared with those from experimental data for Prandtl numbers of 1, 5, 40, 60 and 100, respectively. In the original work of Kato, Nishiwaki and Hirata [4], comparison between theory and experimental data are made for Prandtl numbers of 1 and 40, respectively. The close agreement shown in Figures 2 through 6 further demonstrate the accuracy of this method. Similarly good agreement shown in Fig. 2 and Fig.3 of reference 7 are also observed for the velocity and the temperature profiles.

For the cases of slender cylinders where the effect of transverse curvature is not negligible, numerical solutions are obtained by using the integral method outlined above for a few values of ξ, namely,

$\xi = 0.01, 0.1, 1.0, 10$

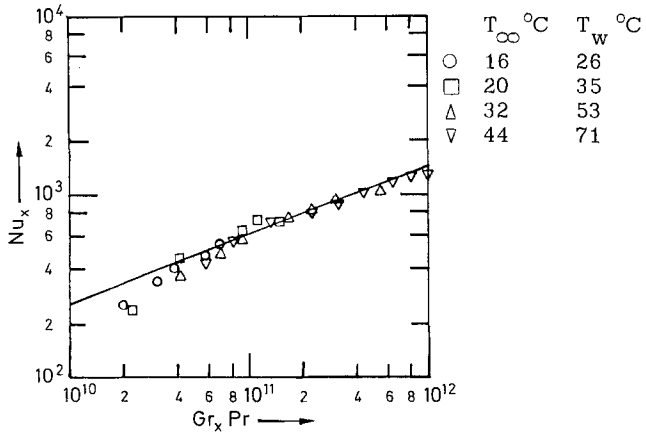

Fig.3. Experimental data (6) vs theoretical results base on present method (Pr = 5.0)

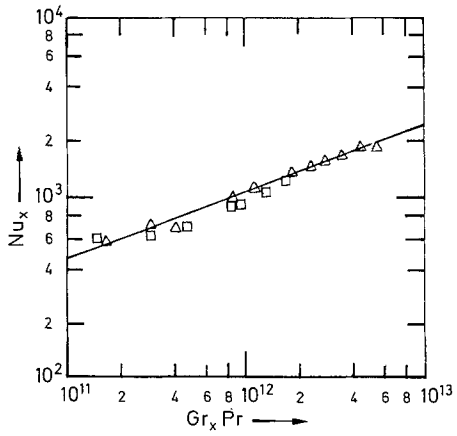

Fig.5. Experimental data (6) vs theoretical results based on present method (Pr = 60)

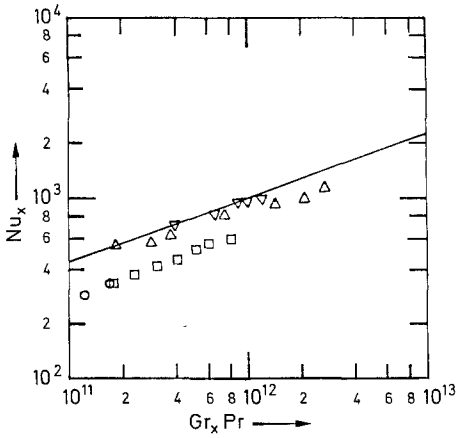

Fig.6. Experimental data (6) vs theoretical results based on present method (Pr = 100)

and for Prandtl numbers of 0.7, 1, 10 and 100 respectively Table 1 through Table 4 give Nu_x as a function of Ra_x, each for a family of values of the transverse curvature parameter ξ. The results are also plotted in Fig.7 for the case of Pr = 1, based on the data of Table 2. The results show clearly that the effect of transverse curvature is to increase the Nusselt number. This is in agreement with the conclusions obtained for laminar natural convection flow over slender cylinders [2]. The same trend is observed for all other Prandtl numbers, as seen from the data given in Table 1 through Table 4. Figures such as Fig.7 for other Prandtl numbers can easily be plotted based on the data shown in these tables. Inspection of Tables 1 through Table 4 shows that the

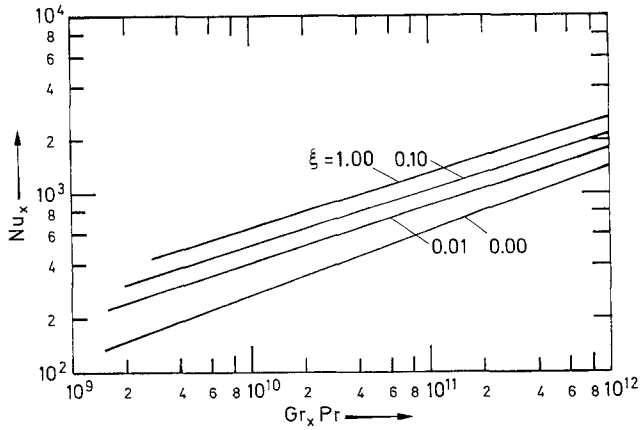

Fig.7. Effect of Transverse Curvature for Pr = 1.0

effect of transverse curvature is more pronounced for smaller Prandtl numbers.

For the turbulent natural convection of a given fluid (β, ν, k and Pr are known) over a given slender cylinder (r_0 is known) with known surface temperature (T_w) and temperature of the surrounding fluid (T_∞), we can calculate Gr_0 by

$$Gr_0 = \frac{g\beta(T_w - T_\infty)r_0^3}{\nu^2}$$

from which the transverse curvature parameter can be calculated by

$$\xi = Gr_0^{-\frac{1}{3}}$$

With ξ known, the method outlined in this paper can be followed and a Nu_x - vs - Ra_x curve, such as the one shown in Fig.7 can then be generated. From the definition of Ra_x,

$$Ra_x = Gr_x\, Pr = \frac{g\beta(T_w - T_\infty)x^3}{\nu^2} \cdot \frac{\mu c_p}{k}$$

it is seen that all the physical constants are given quantities, except x. Now, if a location x is chosen, Ra_x can be calculated from this expression. From the Nu_x - vs - Ra_x figure, the corresponding value of Nu_x can be found. Based on the definition of Nu_x, namely,

$$Nu_x = \frac{hx}{k} = \frac{q_w x}{(T_w - T_\infty)k}$$

the local heat transfer rate for this location, q_w, can be obtained. The above can be repeated for other locations by changing the values of x.

The method is seen to be very useful in obtaining numerical solutions for turbulent natural convection problems. The results are quite accurate and the method is simple to apply since it involves only integrations.

Due to the apparent lack in both theoretical and experimental works in turbulent natural convection flows for geometries other than the semi-infinite flat plate, the theoretical results presented in this work should be useful.

Table 1. Solutions of Eqs.(1) - (3) for Pr = 0.7

ξ	Ra_x	Nu_x
0.	1.24×10^{9}	124.5
	5.78×10^{9}	213.3
	2.89×10^{10}	379.6
	1.30×10^{11}	660.8
	5.45×10^{11}	1129.6
	2.14×10^{12}	1905.7
0.01	1.37×10^{9}	223.3
	5.43×10^{9}	347.6
	2.17×10^{10}	543.4
	8.68×10^{10}	852.5
	3.48×10^{11}	1341.3
	1.40×10^{12}	2115.1
0.1	1.84×10^{9}	309.5
	7.82×10^{9}	485.3
	3.33×10^{10}	763.2
	1.42×10^{10}	1203.3
	6.06×10^{11}	1901.7
1.0	2.46×10^{9}	458.4
	1.10×10^{10}	719.1
	4.93×10^{10}	1130.7
	2.21×10^{11}	1781.7
	9.89×10^{11}	2813.4

Table 2. Solutions of Eqs.(1) - (3) for Pr = 1

ξ	Ra_x	Nu_x
0.	1.53×10^{9}	137.2
	8.62×10^{9}	252.9
	4.39×10^{10}	456.3
	2.02×10^{11}	804.7
	8.51×10^{11}	1391.8
0.01	1.57×10^{9}	225.2
	6.38×10^{9}	353.6
	2.61×10^{10}	558.2
	1.08×10^{11}	884.6
	4.43×10^{11}	1406.3
	1.83×10^{12}	2240.8
0.10	2.04×10^{9}	303.8
	8.87×10^{9}	480.5
	3.88×10^{10}	762.7
	1.70×10^{11}	1214.4
	7.43×10^{11}	1938.4
	3.24×10^{12}	3100.2
1.0	2.67×10^{9}	440.5
	1.22×10^{10}	696.4
	5.61×10^{10}	1104.4
	2.57×10^{11}	1755.6
	1.18×10^{12}	2797.3

Table 3. Solutions of Eqs.(1) - (3) for Pr = 10

ξ	Ra_x	Nu_x
0.	1.70×10^{10}	303.2
	1.03×10^{11}	582.9
	6.17×10^{11}	1132.5
	3.38×10^{12}	2164.1
0.01	9.27×10^{9}	303.9
	4.32×10^{10}	501.4
	2.09×10^{11}	838.5
	1.02×10^{12}	1414.1
	5.06×10^{12}	2396.9
0.1	9.79×10^{9}	355.1
	4.88×10^{10}	589.9
	2.48×10^{11}	989.3
	1.27×10^{12}	2829.6
1.0	1.12×10^{10}	454.8
	5.82×10^{10}	752.9
	3.05×10^{11}	1254.6
	1.61×10^{12}	2104.4
	8.49×10^{12}	3534.4
10.0	1.31×10^{10}	629.1
	6.99×10^{10}	1033.3
	3.75×10^{11}	1705.5
	2.02×10^{12}	2826.4
	1.09×10^{13}	4701.2

Table 4. Solutions of Eqs.(1) - (3) for Pr = 100

ξ	Ra_x	Nu_x
0.	1.30×10^{11}	488.1
	8.12×10^{11}	934.2
	6.60×10^{12}	1984.7
	4.52×10^{13}	4023.6
	2.83×10^{14}	8036.3
0.01	1.52×10^{11}	566.8
	7.95×10^{11}	975.1
	4.35×10^{12}	1704.3
	2.44×10^{13}	3007.6
0.10	2.66×10^{10}	354.4
	1.40×10^{11}	601.9
	7.67×10^{11}	1040.0
	4.33×10^{12}	1816.6
1.00	1.42×10^{11}	697.3
	8.02×10^{11}	1197.0
	4.58×10^{12}	2071.5
	2.64×10^{13}	3607.8
	1.53×10^{14}	6316.1
10.0	1.55×10^{11}	878.9
	8.84×10^{11}	1491.1
	5.09×10^{12}	2545.6
	2.94×10^{13}	4369.5
	1.71×10^{14}	7537.3

References

1. Sparrow, E.M.; Gregg, J.L.: Laminar Free Convection Heat Transfer From the Outer Surface of a Vertical Circular Cylinder. Trans. ASME, V 78 (1956) 1823
2. Cebeci, T.: Laminar-Free-Convective-Heat Transfer From the Outer Surface of a Vertical Slender Circular Cylinder. 5th International Heat Transfer Conference, Tokyo, Japan, 1974
3. Cebeci, T.; Qasim, J.; Na, T.Y.: Free Convection Heat Transfer From Slender Cylinders Subject to Uniform Wall Heat Flux. Heat and Mass Transfer, 1 (1974) 159-162
4. Kato, H.; Nishiwaki, N.; Hirata, M.: On the Turbulent Heat Transfer by Free Convection From a Vertical Plate. International Journal of Heat and Mass Transfer. 11 (1968) 1117-1125
5. Eckert, E.R.G.; Jackson, T.W.: Analysis of Turbulent Free-Convection-Boundary Layer on Flat Plate. NACA Report 1015 (1951)
6. Fujii, T.; Takeuchi, M.; Fujii, M.; Suzaki, K.; Uehara, H.: Experiments on Natural-Convection Heat Transfer From the Outer Surface of a Vertical Cylinder to Liquids. International Journal of Heat and Mass Transfer. 13 (1970) 753-787
7. Jacob, M.: Heat Transfer. New York: John Wiley (1949)
8. Saunders, O.A.: The Effect of Pressure Upon Natural Convection in Air. Proc. Roy. Soc., Series A, A157 (1936) 278-291
9. Fujii, T.: Experimental Studies of Free Convection Heat Transfer. Bull. J.S.M.E., 2 (1959) 555-558
10. Touloukian, Y.S.; Hawkin, G.A.; Jacob, M.: Heat Transfer by Free Convection From Heated Vertical Surface to Liquids. Trans. ASME, (1948) 13-23

T.Y. Na
Professor of Mechanical Engineering
University of Michigan - Dearborn
Dearborn, Michigan 48128, USA

J.P. Chiou
Professor of Mechanical Engineering
University of Detroit
Detroit, Michigan, 48221, USA

Received May 2, 1980